Engineering Science and Technology, an International Journal xxx (xxxx) xxx

HOSTED BY

ELSEVIER

Contents lists available at ScienceDirect

Engineering Science and Technology, an International Journal

journal homepage: www.elsevier.com/locate/jestch

Full Length Article

An approach for one dimensional periodic arbitrary lithography based on Fourier series

Mahdi Kordi [a], Seyed Mohammad Reza Vaziri [a], Fahimeh Armin [a], Mojtaba Joodaki [a,b,*]

[a] Department of Electrical Engineering, Faculty of Engineering, Ferdowsi University of Mashhad, Mashhad 9177948974, Iran
[b] Department of Electrical Engineering, Jacobs University of Bremen, 28759 Bremen, Germany

ARTICLE INFO

Article history:
Received 17 May 2020
Revised 16 August 2020
Accepted 29 August 2020
Available online xxxx

Keywords:
Interference lithography
Fourier series expansion
Arbitrary patterns

ABSTRACT

In interference lithography, 1-dimensional (1D) Fourier series expansion (FSE) technique can be used to create 1D periodic arbitrary patterns. Since the energy of electric field can change the solubility of photoresist, the required electric field intensity to create the desired pattern should be found. Therefore, in this article, an inequality for the magnitude of electric field on the surface of photoresist is addressed. A solution to this equation is provided with one degree of freedom. Intelligent selection of the parameters corresponding to this degree of freedom enhances the performance of the system seriously. The proposed method confirms that our approach can produce subwavelength resolutions. Based on these achievements, we present a new lithography system that can generate 1D periodic arbitrary patterns.

1. Introduction

Photolithography is a key technique for patterning different parts of electronic devices that can be done with or without masks [5,13]. Since mask production can be very costly and time consuming, recent researches are focused on maskless lithography which has the advantages of decreasing the cost and increasing the flexibility in generating different patterns. Electron-beam [14,11,8,29] and focused ion-beam direct writing [16,17,25], probe tip contact [19,7] and interference lithography [27,3,12,9,2] are different examples of maskless lithography methods. Optical beam lithography is another method of direct writing that in contrast to other writing approaches, can produce 3D patterns [20,1,10,24]. However, with respect to the diffraction limit, the resolution of optical beam lithography cannot reach that of electron beam method. To overcome this limitation, using two optical beams and a new type of photoresist, Gan et al. reached smaller feature sizes in this method [6]. The obtained resolution in their work is comparable to that of electron beam approach. Despite these achievements, all the direct writing techniques suffer from low throughput which is further decreased by improving the resolution. However, due to its accuracy, electron beam direct writing is usually used in mask production. On the other hand, interference lithography is fast and decreases the extra costs due to the simplicity of the system. So far, the proposed methods based on the interference lithography can only produce some special periodic patterns.

Using prisms and mirrors is a common method in interference lithography [21,23]. However, each specific pattern requires an specific design of these components, thus arbitrary patterning is not possible by using prisms or mirrors. In the laser interference lithography, the main point is controlling the propagation directions of the waves, e.g. by using Lloyd's mirrors [26,28]. However, in this article, in addition to controlling this feature, amplitudes and phases of the plane waves have to be adjusted using FSE technique and they must be constructed using the proposed setup.

In contrast to 2D lithography, we have a limited variety of patterns in 1D cases. Although the final aim of our research is realizing a periodic arbitrary 2D lithography, in this paper we have focused on 1D patterns only. Using FSE method, we can construct every periodic arbitrary field distribution using plane waves. In this article, the required waves are produced using a monochromatic light source and a set of beam conditioners. As will be shown later, an inequality on the magnitude of electric field should be solved to find the required magnitudes and phases corresponding to the desired pattern.

In this article, we start with a discussion on the creation of 1D periodic arbitrary patterns. The subsequent section focuses on the relationship between the proposed method resolution and the number of the interfering waves. We continue our discussion with an example on 1D patterns and then a new system is described for realization of this type of lithography.

* Corresponding author.
E-mail addresses: mahdi.kordi@mail.um.ac.ir (M. Kordi), s.vaziri92@mail.um.ac.ir (S.M.R. Vaziri), fahimeh.armin@mail.um.ac.ir (F. Armin), joodaki@um.ac.ir (M. Joodaki).

https://doi.org/10.1016/j.jestch.2020.08.014
2215-0986/

2. 1D periodic arbitrary patterns

Based on Fourier analysis, a y-polarized electric field distribution which is periodic in x direction and constant along y direction, can be expanded as a sum of plane waves as follows:

$$\boldsymbol{E}_y(x,z) = \sum_{m=-M}^{+M} e^{-jk_{x,m}x} e^{-jk_{z,m}z} A(k_{x,m}) \boldsymbol{a}_y, \tag{1}$$

where $A(k_{x,m})$ is the amplitude of the corresponding electric field component. By assuming T_x as the periodicity of this field in x direction, we have $k_{x,m} = 2m\pi/T_x$ and

$$k_{z,m} = \begin{cases} \sqrt{k_0^2 - k_{x,m}^2} & k_0^2 \geqslant k_{x,m}^2 \\ -j\sqrt{k_{x,m}^2 - k_0^2} & k_0^2 < k_{x,m}^2, \end{cases} \tag{2}$$

where k_0 is the free-space wavenumber. In order to produce a exact distribution, M should approach to infinity in (1). Also, Eq. (2) guarantees that the Helmholtz equation is satisfied. The propagation direction of each plane wave is obtained by its wave vector, $\boldsymbol{k} = k_{x,m}\boldsymbol{a}_x + +k_{z,m}\boldsymbol{a}_z$. If the photoresist is placed at $z = 0$ plane, the electric field on this surface can be explained as

$$\boldsymbol{E}_y(x,0) = \sum_{m=-M}^{+M} e^{-jk_{x,m}x} A(k_{x,m}) \boldsymbol{a}_y. \tag{3}$$

If $f(x)$ represents the cross section of the desired lithography pattern, in digital lithography, there are only two values for $f(x)$, 1 or 0. To reach the desired pattern at a specific exposure time, the intensity of electric field, $|\boldsymbol{E}_y(x,0)|$, should be greater than a threshold value (E_{th}) for areas with $f(x) = 1$. In this article, we consider the areas with $f(x)$ of 1 as "on" regions. On the other hand, if $f(x) = 0$, the statement $|\boldsymbol{E}_y(x,0)| < E_{th}$should be satisfied and we consider the corresponding areas as "off" regions. Therefore, the intensity of electric field should satisfy the following conditions

$$|\boldsymbol{E}_y(x,0)| = g(x) \begin{cases} > E_{th} & f(x) = 1 \\ < E_{th} & f(x) = 0. \end{cases} \tag{4}$$

With respect to Eq. (4), only the magnitude of y component of the electric field should be greater than E_{th} in the "on" regions with no constraint on its phase. So, we have

$$E_y(x,0) = g(x) e^{j\varphi(x)}, \tag{5}$$

where $\varphi(x)$ is an arbitrary real function. Eq. (5) introduce one degree of freedom in the solution. A simple but not necessarily the optimum solution to this equation is

$$\begin{cases} g(x) = \alpha f(x) \\ \varphi(x) = 0, \end{cases} \tag{6}$$

where α is a constant. With respect to the threshold value, α must be chosen in a way that the final pattern is as close as the desired one. Eqs. (3) and (5) yield to

$$A(k_{x,m}) = \frac{1}{T_x} \int_{x=-\frac{T_x}{2}}^{\frac{T_x}{2}} g(x) e^{j\varphi(x)} e^{jk_{x,m}x} dx. \tag{7}$$

3. Interference and resolution

With respect to Eq. (2), there are two different sets of plane waves [18]. In this equation, the condition of $k_0^2 \geqslant k_{x,m}^2$ corresponds to propagating waves, while $k_0^2 < k_{x,m}^2$ corresponds to evanescent waves. To have an arbitrary pattern, the required plane waves should be excited. Using devices with high numerical apertures, the evanescent waves can be produced through the total internal reflection phenomenon [22]. However, the main limitation for creation of the evanescent waves is their rapid attenuation in the photoresist layer. Although this challenge can be downgraded using effective gain media [15], the practical implementation of such ideas, especially control of their magnitudes and phases, is more difficult. Hence, in our proposed setup we only focus on producing the propagating waves that will be described later.

If $T_x/\lambda < 1$, the only propagating term participating in the interference is the one with $m = 0$. Therefore, if the evanescent waves are not considered, the period of the created electric field on the photoresist surface should be greater than the wavelength. At the lower bound, $T_x = \lambda$, the created electric field has a cosine form with a period of λ. Since the resulted pattern is related to the squared magnitude of electric field, it can be concluded that the period of the final pattern cannot be smaller than the half wavelength. By only producing propagating waves, we have

$$k_0 \geqslant k_{x,M}, \tag{8}$$

and so, there is a limit on the number of Fourier terms in Eq. (1)

$$M \leqslant \frac{T_x}{\lambda}. \tag{9}$$

In general, to create a more complex pattern, a larger number of interfering waves are needed, which require a larger wavenumber. This argument gives an intuitive insight about the relationship between the number of waves and the lithography resolution. Similar interpretation can be extended to 2D interference lithography.

4. An example on 1D patterns

In the following, an example is presented in order to investigate the capability of our proposed method. The 1D example consists of two strips of different widths in a unit cell with the period of 5λ ($M_{max} = 5$). The widths of the first and second strips are 0.5λ and 0.8λ, respectively. The desired lithography pattern is

$$f(x) = \begin{cases} 1 & -1.3\lambda < x < -0.8\lambda \\ 1 & 0.5\lambda < x < 1.3\lambda \\ 0 & otherwise, \end{cases} \tag{10}$$

and is shown by the hatched areas in Fig. 1(a). The parameters used in our calculations are as follows:

$$\begin{cases} M = M_{max} = 5, \\ g(x) = 2.32 \times f(x), \\ \varphi(x) = 0, \\ E_{th} = 1. \end{cases} \tag{11}$$

The normalized intensity squared of resulted electric field along the x axis is represented in Fig. 1(a) with pink dashed line. According to the threshold value (green line), the width of the second strip is narrower than the desired one. Our proposed solution to this problem is to modify $g(x)$ as follows:

$$g_1(x) = 2.377 \times \begin{cases} 1 & -1.3\lambda < x < -0.8\lambda \\ 1 & 0.425\lambda < x < 1.35\lambda \\ 0 & otherwise. \end{cases} \tag{12}$$

As can be seen in Fig. 1(a) (black line), the width of both strips are as desired ones by this modification. Specifications of the required plane waves for realization of the desired pattern $f(x)$ are calculated using Eq. (7) and summarized in Table 1.

Fig. 1(b) shows the field distribution corresponds to the function $g_1(x)$. In this figure, a strip with the width of 0.5λ is easily realized. This result confirms the ability of our method in producing

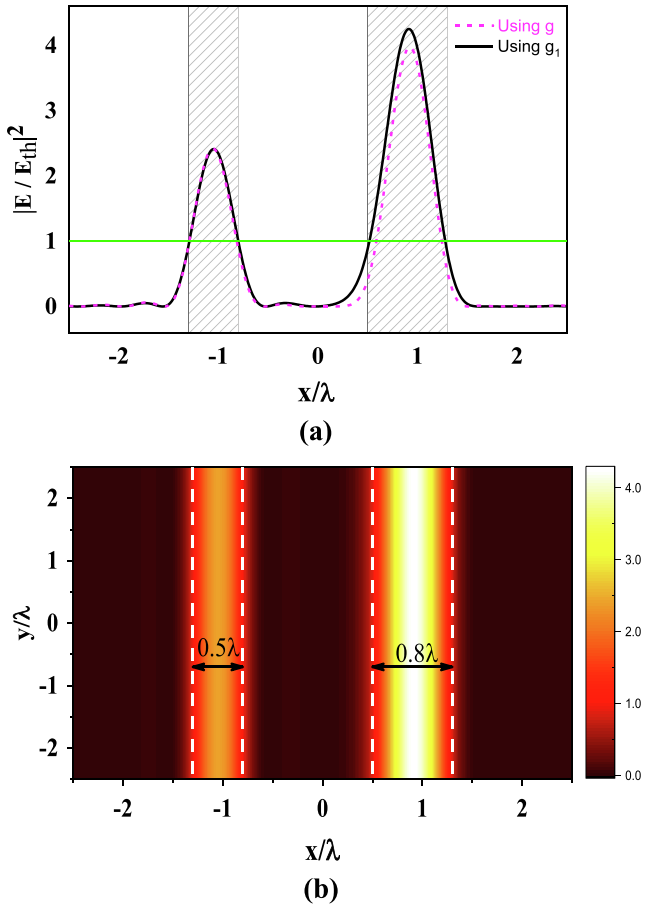

Fig. 1. (a) The square of normalized electric field intensity along the x axis. The green line corresponds to the threshold value and the hatched areas show the "on" regions. (b) The square of normalized electric field intensity by using g_1 for the unit cell consisting two strips with different widths. The white dashed lines show the boundaries of the desired pattern.

the desired patterns with subwavelength resolution. The obtained resolution can be even improved by implementing an optimization process.

It is worth mentioning that an appropriate selection of the function corresponding to Eq. (5), can improve the performance of the system substantially. More studies are needed on the optimization of this function that can be a new field of research in our lithography system.

5. Creation of the required plane waves

To create an arbitrary pattern, its Fourier terms should be realized using plane waves with specific magnitudes ($|A(k_{x,m})|$), phases ($\angle A(k_{x,m})$) and propagation directions ($\boldsymbol{k} = k_{x,m}\boldsymbol{a}_x + +k_{z,m}\boldsymbol{a}_z$ or its equivalent angle $\phi_m = tan^{-1}\frac{k_{x,m}}{K_{z,m}}$ that is depicted in Fig. 2(b)). The required waves can be produced using a monochromatic source and a number of beam conditioners equal to the number of Fourier terms. A schematic configuration is sketched in Fig. 2 and our proposed beam conditioner is shown in Fig. 2(b).

Table 1
Specifications of the plane waves obtained from the FSE of $g_1(x)$ (given in Eq. (12)). These waves are required for realizing the desired pattern, $f(x)$ (given in Eq. (10)). All of the waves are polarized in y direction. The required θ for creating the corresponding $|A(k_{x,m})|$ is extracted from Fig. 2(b), and written in the last column. In extraction of θ, the maximum magnitude of $|A(k_{x,m})|$ is normalized to 1.

m	$\lvert A(k_{x,m})\rvert$	$\angle A(k_{x,m})$	$\phi_m = Tan^{-1}(\frac{k_{x,m}}{k_{z,m}})$	θ
0	0.479	0	0	70.5
±1	0.199	±31.3	±11.5	76.2
±2	0.311	±157.7	±23.6	71.5
±3	0.279	±165.6	±36.8	75.2
±4	0.046	±16.2	±53.1	89.2

As can be seen in Fig. 2(a), a monochromatic source illuminates the beam conditioners and then, the transmitted waves from them interfere on the surface of photoresist. Thus, the desired field distribution is created on this surface. Transmission coefficient of the light passing through a dielectric slab (T), is dependent on the angle of incidence (θ) and also the height of slab (h). This phenomenon, for which the mathematical relations are presented in [4], is sketched schematically in Fig. 2(c).

With a fixed h, a stepper motor is needed for tuning the angle of θ and consequently, the magnitude of the plane wave. In Figs. 3(a) and (b), the magnitude of transmission coefficient is shown versus the angle θ for two different heights of the slab. The refractive index of the slab is equal to 1.5 ($n = 1.5$) in calculating the transmission coefficients. As shown in these figures, the number of fluctuations increases for a larger height. Therefore if the height of the slab is increased, for accurate controlling of the plane wave magnitude, a step motor with finer step resolution is needed. For example in Fig. 3(a) and (b), in order to change the magnitude of transmission coefficient by one percent, the step motor resolution should be around 0.1° and .03° for $h = 10\lambda$ and $h = 30\lambda$, respectively. Also, to realize the magnitudes of Table 1 using a dielectric slab with $h = 30\lambda$ and $n = 1.5$ (Fig. 3(b)), the corresponding angles of incidence (θ) are extracted from Fig. 3(b)), and written in the last column of this table.

Another way to control the magnitude is changing the slab height for a fixed angle θ. The magnitude of transmission coefficient versus height of the slab is shown in Fig. 3(c) where $\theta = 75°$ and $n = 1.5$. For this purpose, a piezoelectric slab can be used for fine adjusting the height in the range of a few nanometers and even lower values. Also, changing the refractive index n can also control the transmission coefficient with fixed θ and h. This can be done using materials with Pockels effect.

As can be seen in Fig. 2(b), we have used a dielectric slab and a mirror as our proposed beam conditioner. The phase change of the wave from the source to the surface of photoresist is obtained from

$$\Delta\varphi = k_0 l_1 + \varphi(T) + k_0(l_2 + l_3) \tag{13}$$

where l_1, l_2 and l_3 are the distances from the source to the slab, slab to the mirror, and mirror to the surface of photoresist, respectively. These distances are depicted in Fig. 2(b). Also, $\varphi(T)$ is the phase of the transmission coefficient T, which depends on θ and h. By assuming that all the dielectric slabs are placed on the same level, l_1 is constant for all of them. Therefore, based on the Eq. (13) and considering $\varphi(T)$, the total phase can be tuned by displacement of the mirror in z direction. this can be done with a piezoelectric slab (the distance $l_2 + l_3$ is changed by this displacement). Also, the propagation directions of plane waves that are determined by their wave vectors, can be adjusted by the orientation of the corresponding mirrors that can be done with a stepper motor.

As a consequence, if we control the magnitude of the plane wave by changing θ, the requirements of the proposed beam conditioner are a dielectric slab, a mirror, two stepper motors and a piezoelectric slab for the mirror displacement. However, if the magnitude of plane wave is controlled by changing the slab height, the corresponding requirements are a piezoelectric slab, a mirror, a stepper motor and another piezoelectric slab for the mirror displacement. Albeit, there may be other approaches to realize the required plane waves and each of them needs its special requirements. Hence, by implementing the setup depicted in Fig. 2(b), a

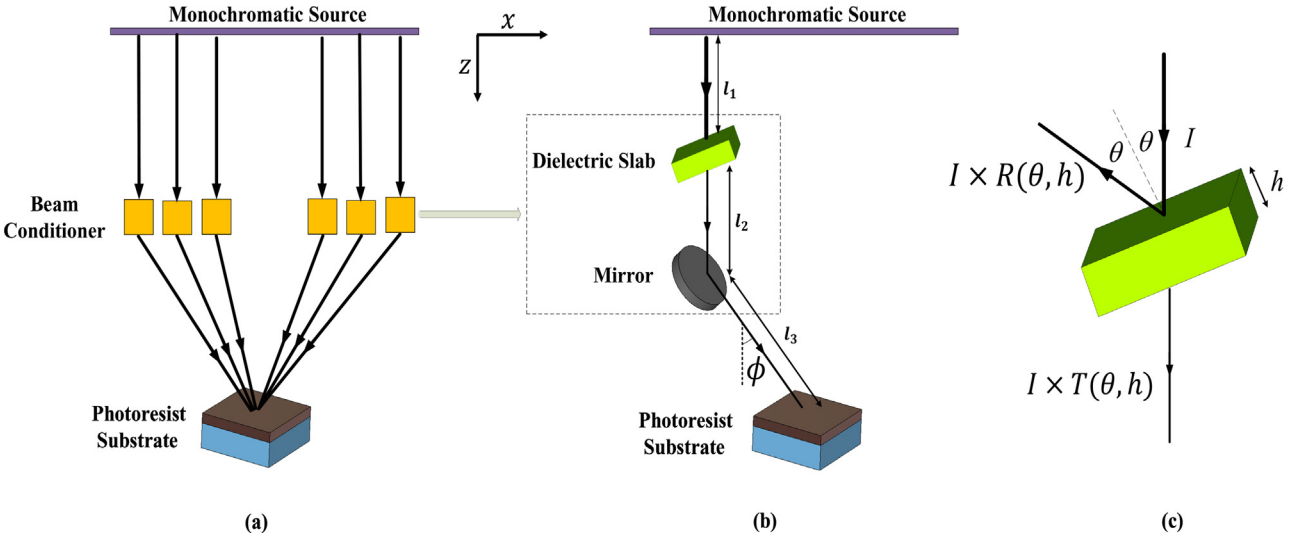

Fig. 2. (a) The general schematic configuration of the proposed interference lithography system. (b) The proposed beam conditioner. (c) The schematic representation of light passing thorough the dielectric slab with $T(\theta, h)$ and $R(\theta, h)$ as the transmission and reflection coefficients, respectively.

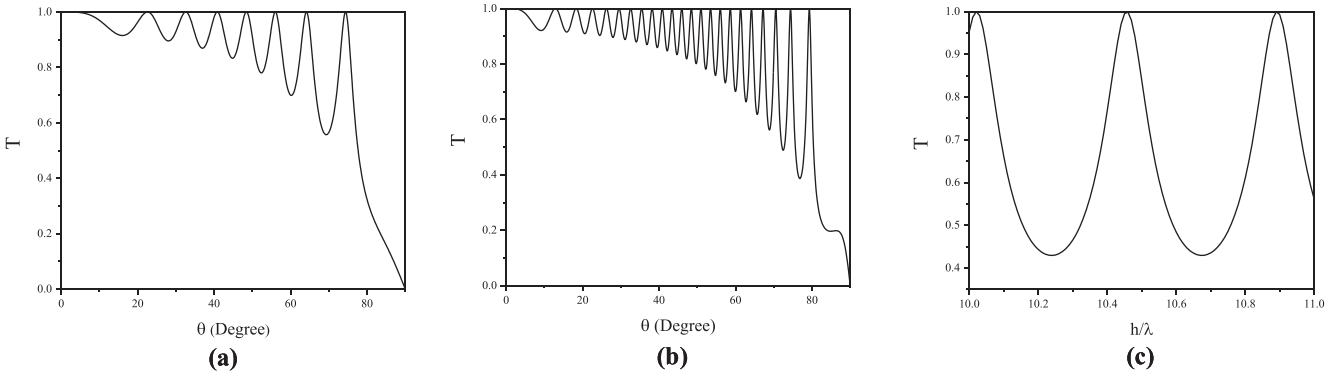

Fig. 3. The magnitude of transmission coefficient versus the incident angle θ for two different heights of the slab (a) $h = 10\lambda$ and (b) $h = 30\lambda$. (c) The magnitude of transmission coefficient versus variation of the height of the slab where $\theta = 75^{\circ}$. The refractive index of slab is $n = 1.5$. TE polarization is assumed for calculating all the transmission coefficients.

plane wave with arbitrary magnitude, phase and propagation direction can be produced.

There are some practical challenges in the realization of our proposed setup that must be considered. For example, any error in adjusting the specifications of the beam conditioners affects the performance of our lithography system. Errors in θ or the slab height, h, leads to a wrong amplitude of the plane waves. Also, if the substrate is not perfectly horizontal or if the mirrors orientation is not accurately adjusted, the produced angle ϕ_m deviates from its desired value. This leads to a small variation in the value of $k_{x,m} = k_0 \times cos(\phi_m)$ in Eq. (3). As a consequence, a calibration system is strongly needed for tuning the magnitudes and phases of the plane waves and also one has to deeply investigate the effects of variations in $k_{x,m}$ of Eq. (3) on the performance of the proposed system. Another point that should be considered, is the distortions which might be caused by photoresist especially if the photoresist is thick. Detailed study of these issues is beyond the scope of this article and will be addressed in our future works. This paper mainly focuses on the first proof of the concept.

6. Conclusion

In conclusion, analytical calculations based on FSE technique are used to obtain 1D arbitrary patterns through interference lithography. The outcome of solving the resulted equations are magnitudes, phases and propagation directions of the plane waves required for the desired interference on the photoresist surface. Because the control of the magnitudes and phases of the evanescent waves are difficult, we neglect them in our proposed setup. This can degrade the accuracy of our approach, however, when the number of propagating waves is large enough, the harmful effect of neglecting the evanescent waves can be downgraded and consequently, an acceptable result for the lithography is obtained. For example, the resulted pattern in the Section 4 confirms that a successful lithography can be achieved, even when the evanescent waves are ignored. It should be noted that, our derivations lead to one degree of freedom (Eq. (5)) that helps to reduce the error caused by the finite number of Fourier terms. Thus, optimization of $g(x)$ and $\varphi(x)$ is the next step in our proposed lithography process.

Since proposed approach can create 1D patterns with subwavelength resolution, some 2D patterns with a minimum feature size lower than the wavelength can be obtained by combining double patterning techniques and using our 1D approach. This can be a big step in fabrication of nano-scale devices.

To realize our approach, we present a new embodiment which can be implemented by passive commercial devices. Some challenges in realizing our proposed setup are mentioned and also,

we have some difficulties in finding the monochromatic source. Nevertheless, we should have in mind that our setup does not need a uniform plane wave over all of the beam conditioners. In fact, we need a local uniform plane wave on each beam conditioner and also a calibration system for tuning the magnitudes and phases of the waves. These practical challenges will be considered in our future works. As another future step in our research is developing our approach for 2D periodic arbitrary patterns.

Declaration of Competing Interest

The authors declare that they have no known competing financial interests or personal relationships that could have appeared to influence the work reported in this paper.

References

[1] S. Bagheri, K. Weber, T. Gissibl, T. Weiss, F. Neubrech, H. Giessen, Fabrication of square-centimeter plasmonic nanoantenna arrays by femtosecond direct laser writing lithography: effects of collective excitations on seira enhancement, ACS Photon. 2 (2015) 779–786.
[2] S. Behera, J. Joseph, Design and realization of functional metamaterial basis structures through optical phase manipulation based interference lithography, J. Opt. 19 (2017) 105103.
[3] J. de Boor, D.S. Kim, V. Schmidt, Sub-50 nm patterning by immersion interference lithography using a littrow prism as a lloyd's interferometer, Opt. Lett. 35 (2010) 3450.
[4] M. Born, E. Wolf, Principles of Optics: Electromagnetic Theory of Propagation Interference and Diffraction of Light, Pergamon Pr, 1981.
[5] S.A. Campbell, The Science and Engineering of Microelectronic Fabrication, Oxford, 2001.
[6] Z. Gan, Y. Cao, R.A. Evans, M. Gu, Three-dimensional deep sub-diffraction optical beam lithography with 9nm feature size. Nature, Communications 4 (2013).
[7] D.S. Ginger, H. Zhang, C.A. Mirkin, The evolution of dip-pen nanolithography, Angew. Chem. Int. Ed. 43 (2004) 30–45.
[8] N.A.A. Hatab, J.M. Oran, M.J. Sepaniak, Surface-enhanced raman spectroscopy substrates created via electron beam lithography and nanotransfer printing, ACS Nano 2 (2008) 377–385.
[9] Y. Hou, Z. Wang, Y. Hu, D. Li, R. Qiu, Capture and sorting of multiple cells by polarization-controlled three-beam interference, J. Opt. 18 (2016) 035401.
[10] L. Jonušauskas, S. Juodkazis, M. Malinauskas, Optical 3d printing: bridging the gaps in the mesoscale, J. Opt. 20 (2018) 053001.
[11] T. Kjellberg, R. Schatz, The effect of stitching errors on the spectral characteristics of DFB lasers fabricated using electron beam lithography, J. Lightwave Technol. 10 (1992) 1256–1266.
[12] A. Langner, B. Paivanranta, B. Terhalle, Y. Ekinci, Fabrication of quasiperiodic nanostructures with EUV interference lithography, Nanotechnology 23 (2012) 105303.
[13] G.S. May, S.M. Sze, Fundamentals of Semiconductor Fabrication, Wiely, 2004..
[14] J. McInerney, M. Fice, H. Ahmed, Formation of micrograting for III-v semiconductor integrated optoelectronics by high-voltage electron-beam lithography, J. Lightwave Technol. 4 (1986) 1494–1501.
[15] P. Mehrotra, C.A. Mack, R.J. Blaikie, Super-resolution imaging by evanescent wave coupling to surface states on effective gain media, 2012. arXiv:1206.4148..
[16] J. Orloff, Fundamental limits to imaging resolution for focused ion beams, J. Vacuum Sci. Technol. B 14 (1996) 3759.
[17] J. Orloff, M. Utlaut, L. Swanson, High Resolution Focused Ion Beams: FIB and its Applications, Springer, US, 2003.
[18] J.B. Pendry, Negative refraction makes a perfect lens, Phys. Rev. Lett. 85 (2000) 3966–3969.
[19] R.D. Piner, J. Zhu, F. Xu, S. Hong, C.A. Mirkin, dip-pen nanolithography, Science 283 (1999) 661–663.
[20] C. Rensch, S.V. Hell, M. Schickfus, S. Hunklinger, Laser scanner for direct writing lithography, Appl. Opt. 28 (1989) 3754.
[21] R. Sidharthan, V. Murukeshan, Nano-scale patterning using pyramidal prism based wavefront interference lithography, Phys. Proc. 19 (2011) 416–421.
[22] B.W. Smith, Y. Fan, J. Zhou, N. Lafferty, A. Estroff, Evanescent wave imaging in optical lithography, in: D.G. Flagello (Ed.), Optical Microlithography XIX, SPIE, 2006.
[23] H. Takahashi, Y.J. Heo, I. Shimoyama, Scalable fabrication of PEGDA microneedles using UV exposure via a rotating prism, J. Microelectromech. Syst. 26 (2017) 990–992.
[24] C.Y. Wang, J. Gao, X.M. Jin, On-chip rotated polarization directional coupler fabricated by femtosecond laser direct writing, Opt. Lett. 44 (2018) 102.
[25] J. Wang, X. Zhang, Y. Zhou, K. Li, Z. Wang, P. Peddibhotla, F. Liu, S. Bauerdick, A. Rudzinski, Z. Liu, W. Gao, Scalable fabrication of single silicon vacancy defect arrays in silicon carbide using focused ion beam, ACS Photon. 4 (2017) 1054–1059.
[26] P. Wang, Z. Liu, K. Xu, D.J. Blackwood, M. Hong, A.G. Aberle, R. Stangl, I.M. Peters, Periodic upright nanopyramids for light management applications in ultrathin crystalline silicon solar cells, IEEE J. Photovolt. 7 (2017) 493–501.
[27] C. Weiteneder, W. Klaus, H.P. Herzig, Periodic structures with arbitrary shapes recorded by multiple-beam interference, in: E.B. Kley, H.P. Herzig (Eds.), Lithographic and Micromachining Techniques for Optical Component Fabrication II, SPIE, 2003.
[28] S. Xionglin, L. Hongyu, H. Shuang, Q. Lingxuan, L. Xingzhao, The applications of surface plasmons in ga 2 o 3 ultraviolet photodetector, Opto-Electron. Eng. 45 (2018) 170728.
[29] J. Zhang, C. Con, B. Cui, Electron beam lithography on irregular surfaces using an evaporated resist, ACS Nano 8 (2014) 3483–3489.